Development/Plasticity/Repair

Interaction between Telencephalin and ERM Family Proteins Mediates Dendritic Filopodia Formation

Yutaka Furutani,[1,2] Hitomi Matsuno,[1,2] Miwa Kawasaki,[1] Takehiko Sasaki,[3] Kensaku Mori,[4] and Yoshihiro Yoshihara[1,2]

[1]Laboratory for Neurobiology of Synapse, RIKEN Brain Science Institute, Saitama 351-0198, Japan, [2]Core Research Evolutional Science and Technology, Japan Science and Technology Agency, Osaka 560-0082, Japan, [3]Department of Pathology and Immunology, Akita University School of Medicine, Akita 010-8543, Japan, and [4]Department of Physiology, Graduate School of Medicine, The University of Tokyo, Tokyo 113-0033, Japan

Dendritic filopodia are long, thin, actin-rich, and dynamic protrusions that are thought to play a critical role as a precursor of spines during neural development. We reported previously that a telencephalon-specific cell adhesion molecule, telencephalin (TLCN) [intercellular adhesion molecule-5 (ICAM-5)], is highly expressed in dendritic filopodia, facilitates the filopodia formation, and slows spine maturation. Here we demonstrate that TLCN cytoplasmic region binds ERM (ezrin/radixin/moesin) family proteins that link membrane proteins to actin cytoskeleton. In cultured hippocampal neurons, phosphorylated active forms of ERM proteins are colocalized with TLCN in dendritic filopodia, whereas α-actinin, another binding partner of TLCN, is colocalized with TLCN at surface membranes of soma and dendritic shafts. Expression of constitutively active ezrin induces dendritic filopodia formation, whereas small interference RNA-mediated knockdown of ERM proteins decreases filopodia density and accelerates spine maturation. These results indicate the important role of TLCN–ERM interaction in the formation of dendritic filopodia, which leads to subsequent synaptogenesis and establishment of functional neural circuitry in the developing brain.

Key words: **cell adhesion molecule; dendritic filopodia; dendritic spine; ERM; synaptogenesis; telencephalin**

Introduction

Dendritic filopodia are long, thin, headless, and actin-rich protrusions abundantly found in immature neurons (Ziv and Smith, 1996; Fiala et al., 1998). They are dynamic and highly motile structures that facilitate the formation of physical contacts between dendrites and axons (Dailey and Smith, 1996; Dunaevsky et al., 1999; Lendvai et al., 2000). It has been proposed that dendritic filopodia are morphologically and functionally transformed into mature mushroom-shaped spines, although the precise cellular mechanisms of spine formation are still controversial (Yuste and Bonhoeffer, 2004). The mature spines constitute a postsynaptic structure of >90% excitatory synapses in adult mammalian brain (Harris and Kater, 1994). Thus, as a precursor of spine, dendritic filopodia most likely plays a critical role in the formation of functional neural circuitry during development. Additionally, morphological abnormalities of dendritic protrusions are frequently associated with several mental disorders such as fragile X, Down, and Rett syndromes (Kaufmann and Moser, 2000). However, little is known about the molecular mechanisms underlying the formation of dendritic filopodia and the transition from filopodia to spines.

Received March 8, 2007; revised June 14, 2007; accepted July 5, 2007.

This work was supported in part by a Grant-in-Aid for Scientific Research on Priority Areas (Molecular Brain Science; Membrane Traffic) from the Ministry of Education, Culture, Sports, Science, and Technology of Japan (Y.Y.). We thank Dr. Atsushi Miyawaki (RIKEN Brain Science Institute) for Venus cDNA, Tomoko Ito for help in establishment of TLCN-N2a cell line, and members of the Yoshihara laboratory for helpful discussion.

Correspondence should be addressed to Dr. Yoshihiro Yoshihara, Laboratory for Neurobiology of Synapse, RIKEN Brain Science Institute, 2-1 Hirosawa, Wako, Saitama 351-0198, Japan. E-mail: yoshihara@brain.riken.jp.

DOI:10.1523/JNEUROSCI.1047-07.2007

 0270-6474/07/278866-11$15.00/0

Telencephalin (TLCN) [intercellular adhesion molecule-5 (ICAM-5)] is a cell adhesion molecule belonging to the ICAM group of the Ig superfamily (Yoshihara and Mori, 1994; Yoshihara et al., 1994). TLCN is expressed in spiny neurons within the most rostral brain segment, telencephalon, which take charge of higher brain functions such as learning, memory, emotion, consciousness, integration of sensory information, and control of voluntary movements (Mori et al., 1987; Oka et al., 1990; Mitsui et al., 2007). In the telencephalic neurons, TLCN is specifically localized to dendrites but not to axons (Benson et al., 1998; Mitsui et al., 2005). Ontogenic appearance of TLCN parallels the timing of dendritic outgrowth, spine formation, and synaptogenesis in early postnatal life, and the expression persists into adulthood (Mori et al., 1987; Yoshihara and Mori, 1994; Yoshihara et al., 1994). Recently, we reported that TLCN facilitates the formation and maintenance of dendritic filopodia and thereby slows spine maturation in hippocampal neurons (Matsuno et al., 2006). This function of TLCN requires both its extracellular and cytoplasmic regions, suggesting the involvement of unknown ligands/counter-receptors and cytoskeleton-associated intracellular binding partners in TLCN-mediated morphogenesis of dendritic filopodia.

In this study, we performed yeast two-hybrid screening to search for molecules that interact with the cytoplasmic region of TLCN and identified ezrin, radixin, and moesin, so-called ERM family proteins, as specific intracellular binding partners for TLCN. ERM proteins are adaptor molecules that link membrane proteins to actin cytoskeleton and mediate formation of unique membrane-protruding structures such as microvilli, uropods, and membrane ruffles (Tsukita and Yonemura, 1999; Bretscher

et al., 2002). Here we demonstrate for the first time that ERM proteins mediate the formation of dendritic filopodia in developing neurons and that the interaction between TLCN and ERM proteins plays a key role in dendritic morphogenesis and subsequent synaptogenesis.

Materials and Methods

Antibodies. Primary antibodies used in this study were as follows: guinea pig anti-mouse TLCN/Fc (1:1000) (Matsuno et al., 2006); rabbit anti-phospho-ERM (1:100; Cell Signaling Technology, Beverly, MA); mouse anti-α-actinin and mouse anti-FLAG M2 (1:400 and 1:10000, respectively; Sigma, St. Louis, MO); and rat anti-green fluorescent protein (GFP) (1:1000; Nacalai Tesque, Kyoto, Japan). Cyanine 3 (Cy3)- and Cy5-conjugated secondary antibodies were purchased from Jackson ImmunoResearch (West Grove, PA). Alexa488-conjugated secondary antibodies were purchased from Invitrogen (Carlsbad, CA).

Yeast two-hybrid analyses. Yeast two-hybrid screening was performed by Hybrigenics (Paris, France). TLCN cytoplasmic region (TLCN-CR) (amino acids 859–917) was PCR amplified and cloned in a yeast two-hybrid vector optimized by Hybrigenics. The bait construct was transformed in the L40 galactosidase-4 yeast strain (Fromont-Racine et al., 2002). A rat hippocampus random-primed cDNA library, transformed into the Y187 yeast strain and containing 10 million independent fragments, was used for mating. High mating efficiency was obtained by using specific mating method (Fromont-Racine et al., 2002). The screen was first performed on a small scale to adapt the selective pressure to the intrinsic property of the bait. Neither toxicity nor autoactivation of the bait was observed. Thus, the full-scale screen was performed in conditions ensuring a minimum of 50 million interactions tested, to cover five times the primary complexity of the yeast-transformed cDNA library (Rain et al., 2001). Sixty-eight million interactions were actually tested with TLCN cytoplasmic region. After selection on medium lacking Leu, Trp, and His, 15 positive clones were picked, and corresponding prey fragments were amplified by PCR and sequenced at their 5′ and 3′ junctions. Sequences were compared with the GenBank database using BLASTN.

The interactions between TLCN and ERM proteins were confirmed by yeast two-hybrid assays according to the instruction of the manufacturer (DupLEX-A yeast two-hybrid system; OriGene Technologies, Rockville, MD). TLCN-CR (amino acids 859–917) and ICAM-2-CR (amino acids 250–277) were PCR amplified and cloned into *Eco*RI/*Bam*HI site of pEG202. cDNA fragments encoding ezrin, radixin, moesin, merlin, band 4.1, and talin FERM domains were subcloned into *Eco*RI/*Xho*I sites of pJG4–5 vector to generate pJG4–5–ezrin–FERM, pJG4–5–radixin–FERM, pJG4–5–moesin–FERM, pJG4–5–merlin–FERM, pJG4–5–band 4.1–FERM, and pJG4–5–talin–FERM. Individual pEG202 plasmid constructs [pEG202 (negative control), pEG202–TLCN-CR, and pEG202–ICAM-2-CR] were transformed into EFY48 yeast strain together with each pJG4–5–FERM domain plasmid. Interactions between the cytoplasmic region of TLCN (or ICAM-2) and the FERM domains of various molecules were assessed by the growth capability of transformants on Leu^- plates and by the expression of β-galactosidase activity.

Recombinant proteins. cDNA fragments encoding ezrin, radixin, moesin, merlin, band 4.1, and talin FERM domains were subcloned into *Eco*RI/*Xho*I sites of pGEX4T1 vector (GE Healthcare, Piscataway, NJ) to generate pGEX–ezrin–FERM, pGEX–radixin–FERM, pGEX–moesin–FERM, pGEX–merlin–FERM, pGEX–band 4.1–FERM, and pGEX–talin–FERM. *Escherichia coli* BL21 LysS (Invitrogen) was transformed with these plasmids. Expression and purification of fusion proteins consisting of glutathione *S*-transferase (GST) and FERM domains were performed according to the instruction of the manufacturer. Purity of the recombinant proteins was >85% as assessed by SDS-PAGE and Coomassie Brilliant Blue R-250 staining.

Surface plasmon resonance analysis. Direct binding kinetics between TLCN and ERM proteins was determined by surface plasmon resonance analysis (Biacore 2000; Biacore, Uppsala, Sweden). The following N-terminally biotinylated peptides were synthesized: TLCN–CP1 (QSTACKKGEYNVQEAESSGEAV), TLCN–CP2 (GEAVCLNGAGGTPGAEGGAE), TLCN–CP3 (GGAETPGTAESPADGEVFAIQLTSS), mutated TLCN–CP1 (QSTAC*AA*GEA*N*AQEAESSGEAV), and ICAM-2–CP1 (HWHRRRTGTYGVLAAWRRLPRA). The peptides were coupled to streptavidin-coated sensor surfaces (Sensor Chip SA). The FERM domain–GST fusion proteins were serially diluted in running buffer [10 mM HEPES, pH 7.4, containing 150 mM NaCl, 1 mM EDTA, 1 mM DTT, 0.05% (v/v) Tween-20] and injected at a 10 μl/min flow rate. Surface regeneration was performed by injection of 10 mM glycine-HCl, pH 2.0. Relative binding was measured as an increase in arbitrary response units, and kinetic parameters were calculated using the BIAevaluation 3.0 software.

Transfection of N2a cells. N2a cells were maintained in DMEM supplemented with 10% fetal bovine serum (FBS) at 37°C in a humidified atmosphere containing 5% CO_2. cDNA encoding a variant of yellow fluorescent protein (YFP) with fast and efficient maturation, Venus (Nagai et al., 2002), was fused to a membrane-anchoring palmitoylation signal of GAP-43 and subcloned into pCAGGS vector (Niwa et al., 1991) to generate pCAG–gapVenus (Matsuno et al., 2006). Phospholipase C δ1 (PLCδ1)-pleckstrin homology (PH), tandem PH domain-containing protein 2 (TAPP2)-PH, and early endosomal antigen 1 (EEA1) FYVE domains (Balla and Varnai, 2002; Marshall et al., 2002) were fused to enhanced GFP (Takara, Kyoto, Japan) and subcloned into pCAGGS vector to produce pCAG–PLCδ1-PH–GFP, pCAG–TAPP2-PH–GFP, and pCAG–EEA1–3×–FYVE–GFP. N2a cells were transfected with the expression plasmids using Lipofectamine 2000 (Invitrogen).

Establishment of TLCN-inducible N2a cell line. For inducible expression of TLCN in N2a cells, we used the LacSwitch Inducible Mammalian Expression System (Stratagene, La Jolla, CA). Mouse TLCN cDNA was subcloned into the *Not*I site of pOPRSVICAT vector containing the modified *lac* operon sequences, generating pOPRSVI–TLCN. N2a cells were sequentially transfected with two plasmids, pOPRSVI–TLCN and p3SS (a plasmid containing the *lac*-repressor and hygromycin-resistant gene), according to the instruction of the manufacturer. After selection in medium supplemented with 400 μg/ml G418 and 200 μg/ml hygromycin, resistant colonies were picked. Individual clones were screened for isopropyl-β-D-thiogalactopyranoside (IPTG)-induced expression of TLCN by Western blot analysis using anti-TLCN-C antibody which recognize the C-terminal cytoplasmic sequence of TLCN (Matsuno et al., 2006). One stable line was established that showed the highest level of TLCN expression during IPTG treatment.

Expression of constitutively active ezrin in cultured hippocampal neurons. Hippocampal neuronal cultures were prepared from mice at embryonic day 16 as described previously (Okabe et al., 1999). Dissociated cells were plated on poly-L-lysine-coated cover glasses at a very low density (7.0×10^4 cells/35-mm-diameter dish) and maintained in MEM containing 2% B27 supplement (Invitrogen), 5% FBS, and 0.5 mM glutamine. Cytosine β-D-arabinofuranoside was added at the final concentration of 10 μM after 60 h of plating. cDNAs encoding mouse constitutively active form of ezrin (T567D) (Gautreau et al., 2000) and ezrin FERM domain (amino acids 1–312) were PCR amplified and subcloned into *Eco*RI/*Xba*I sites of pFLAG-CMV14 vector (Sigma) to generate pCMV–ezrin–T567D and pCMV–ezrin–FERM, respectively. Injection of these expression plasmids into the cultured neurons was performed as described previously (Matsuno et al., 2006).

Small interference RNA-mediated knockdown of ERM proteins. Nucleotide sequences of small interfering RNA (siRNA) for ERM knockdown were designed as follows: ezrin, 5′-GAT CCG CAA GAT TCA TTG TCA CTG TTC AAG AGA CAG TGA CAA TGA ATC TTG CTT TTT TGG AAA-3′ and 5′-AGC TTT TCC AAA AAA GCA AGA TTC ATT GTC ACT GTC TCT TGA ACA GTG ACA ATG AAT CTT GCG-3′; radixin, 5′- GAT CCG CTA AAT TCT TTC CTG AAG TTC AAG AGA CTT CAG GAA AGA ATT TAG CTC TTT TTT GGA AA-3′ and 5′-AGC TTT TCC AAA AAA GAG CTA AAT TCT TTC CTG AAG TCT CTT GAA CTT CAG GAA AGA ATT TAG CG-3′; moesin, 5′-GAT CCG CCT AGC TCT CTA GAA TAG ATT CAA GAG ATC TAT TCT AGA GAG CTA GGT TTT TTG GAA A-3′ and 5′- AGC TTT TCC AAA AAA CCT ACG AGA GTA CAT ATC ATC TCT TGA ATG ATA TGT ACT CTC GTA GGC G-3′; negative control (mismatched ezrin), 5′- GAT CCT CAA CAT TGA TAC AGT GAC TTC AAG AGA GTC ACT GTA TCA ATG TTG

ATT TTT TGG AAA-3′ and 5′- AGC TTT TCC AAA AAA TCA ACA TTG ATA CAG TGA CTC TCT TGA AGT CAC TGT ATC AAT GTT GAG-3′. Complementary oligonucleotides were annealed and inserted into *Bam*HI/*Hin*dIII sites of pSilencer 3.0-H1 vector containing RNA polymerase III promoter (Ambion, Austin, TX). The siRNA-expressing plasmids were transfected into N2a cells or injected into cultured hippocampal neurons. The expression levels of ezrin, radixin, and moesin were analyzed by quantitative PCR and Western blotting for N2a cells and by immunostaining for cultured hippocampal neurons (supplemental Fig. 1, available at www.jneurosci.org as supplemental material).

Immunoprecipitation. TLCN-inducible N2a cells were transfected with pFLAG–CMV14 or pCMV–ezrin–FERM. After 24 h of the transfection, 10 mM IPTG was added for the induction of TLCN, and the cells were further incubated for 48 h. The cells were lysed with 50 mM Tris-HCl, pH 7.5, containing 1% NP-40, 150 mM NaCl, and Complete Protease Inhibitor Cocktail (Roche Molecular Biochemicals, Mannheim, Germany). The lysates were passed through a 22 gauge syringe needle and centrifuged at 18,000 × *g* for 15 min at 4°C. The supernatants (1 mg of protein) were combined with 10 μg of anti-TLCN/Fc antibody and 20 μl of Protein A-Sepharose (GE Healthcare) and mixed for 3 h. The immunoadsorbents were recovered by centrifugation for 1 min at 700 × *g* and then washed five times by resuspension and centrifugation (1 min at 700 × *g*) in lysis buffer. The samples were boiled in 60 μl of SDS sample buffer containing 50 mM dithiothreitol and subjected to Western blot analysis using anti-FLAG M2 antibody.

Immunocytochemistry. N2a cells and neurons were fixed with 4% paraformaldehyde or 10% TCA, permeabilized with 0.25% Triton X-100 in PBS, blocked with 10% goat serum, incubated with primary antibodies overnight, and then treated with Cy3-, Cy5-, or Alexa488-labeled secondary antibodies.

Image acquisition and statistical analysis. Fluorescent images were acquired using Fluoview FV1000 confocal laser scanning microscopy (Olympus Opticals, Tokyo, Japan). Measurement of spine and filopodia densities was performed as described previously (Matsuno et al., 2006). Dendritic spines and filopodia were determined by the following criteria: spines are defined as protrusions of 0.5–1.5 μm length that had distinct mushroom-shaped head, and filopodia are defined as filamentous protrusions longer than 1.5 μm. Densities of spines and dendritic filopodia were indicated as the number per 10 μm dendritic length.

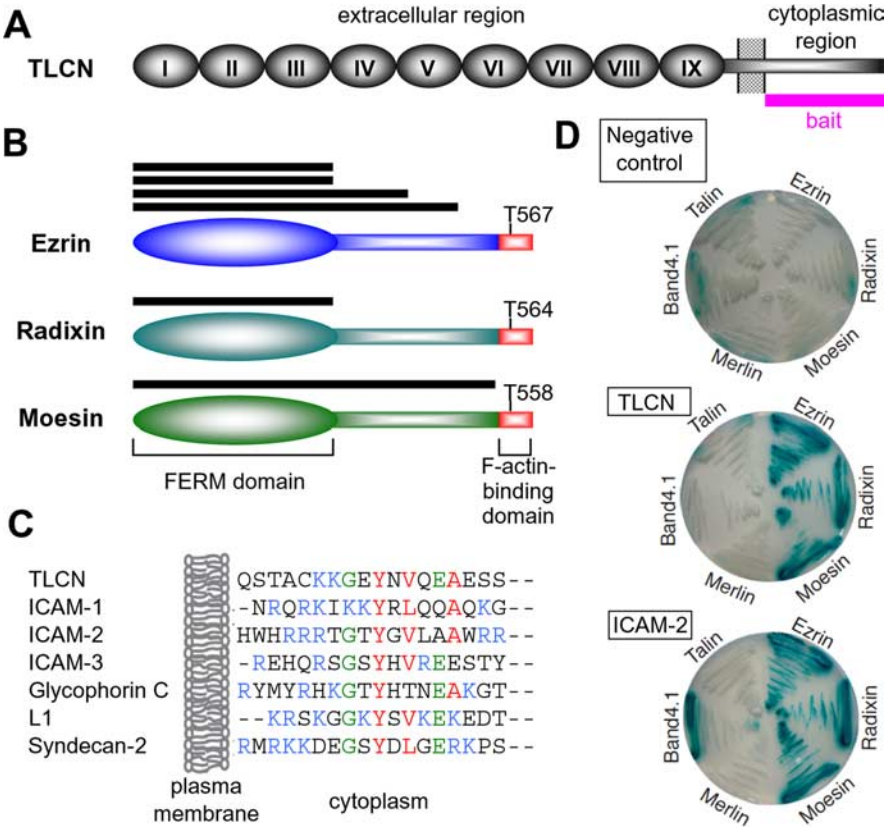

Figure 1. TLCN cytoplasmic region binds to ERM proteins. ***A***, A schematic diagram depicting the structure of TLCN. Roman numbers indicate nine Ig-like domains in the extracellular region. A whole cytoplasmic region used as a bait for yeast two-hybrid screening is shown as a magenta bar. ***B***, Structures of ezrin, radixin, and moesin. The N-terminal FERM domains and the C-terminal F-actin-binding domains are shown in ovals and red boxes, respectively. T567, T564, and T568 represent phosphorylation sites (Thr residues) near the C terminus. Horizontal black bars indicate positive clones obtained in the two-hybrid screening, all of which contain the N-terminal FERM domains. ***C***, Amino acid sequence alignment of the juxtamembrane region of representative ERM-binding proteins. Hydrophobic residues important for the interaction of ICAM-2 with radixin (Hamada et al., 2003) are shown in red, well conserved Gly and Glu in green, and basic residues in blue. ***D***, Confirmation of the interaction between TLCN and ERM proteins. Yeasts were cotransformed with three expression plasmids: pJGC containing the FERM domain of ezrin, radixin, moesin, merlin, band 4.1 or talin, pEG202 containing TLCN or ICAM-2 cytoplasmic regions or pEG202 (negative control), and a LacZ reporter pSH18–34. Interactions were measured by β-galactosidase activities with 5-bromo-4-chloro-3-indolyl-β-D-galactopyranoside as a substrate.

Results

TLCN cytoplasmic region binds to ERM proteins

We demonstrated previously that TLCN plays a crucial role in the formation and maintenance of dendritic filopodia in developing neurons and that the cytoplasmic region of TLCN is indispensable for its proper functioning (Matsuno et al., 2006). This finding suggests that TLCN activates an intracellular signaling cascade for dendritic filopodia morphogenesis through binding to unknown molecules via its cytoplasmic region. To identify molecules that interact with TLCN cytoplasmic region, yeast two-hybrid screening was performed using the full-length sequence (59 amino acids) of mouse/rat TLCN cytoplasmic region as bait and rat hippocampus cDNA library as prey (Fig. 1*A*). Among 15 colonies that survived on $Leu^-/Trp^-/His^-$ selection plates, six clones contained cDNAs encoding ezrin (four clones), radixin (one clone), and moesin (one clone), so-called ERM family proteins (Fig. 1*B*). ERM proteins are the intracellular adaptor molecules that link plasma membrane proteins to actin cytoskeleton (Tsukita and Yonemura, 1999; Bretscher et al., 2002). They consist of N-terminal FERM domain, C-terminal filamentous actin (F-actin)-binding domain, and coiled-coil domain in-between. All the six ERM cDNAs we obtained in the screening contained the FERM domains that are responsible for the interaction with membrane proteins (Fig. 1*B*).

Several cell adhesion molecules including three members of the ICAM family (ICAM-1–ICAM-3) bind ERM proteins via the well conserved juxtamembrane sequences of their cytoplasmic regions (Fig. 1*C*) (Tsukita and Yonemura, 1999; Bretscher et al., 2002). In the cytoplasmic region of ICAM-2, several amino acid residues important for the binding to radixin FERM domain were determined by x-ray crystallography (Hamada et al., 2003). The amino acid sequence alignment revealed that the juxtamembrane region of TLCN contains all the crucial amino acids identified in ICAM-2 and

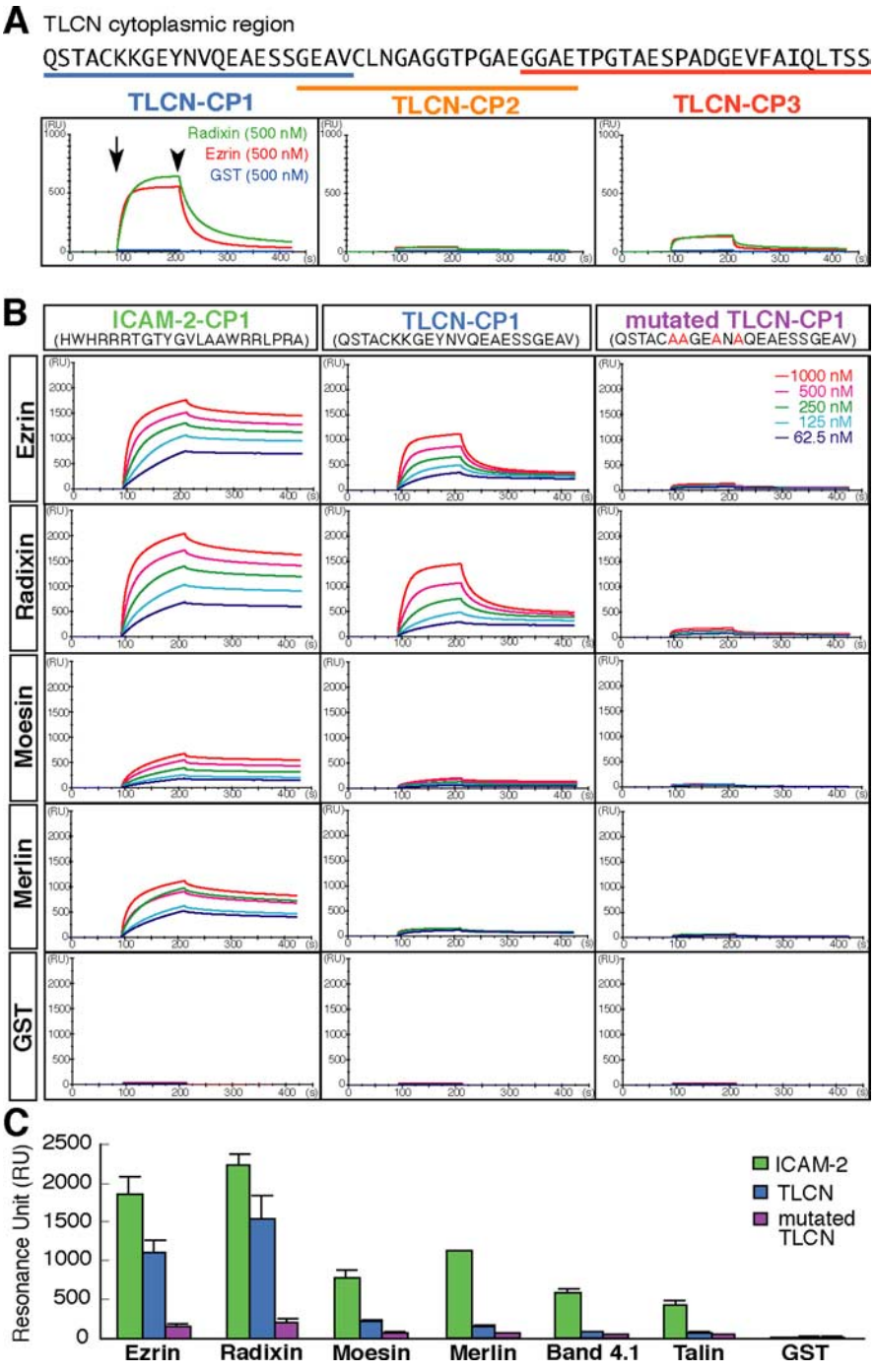

Figure 2. Surface plasmon resonance analysis of binding between TLCN and ERM proteins. ***A***, The amino acid sequence of mouse TLCN cytoplasmic region is shown with three synthetic peptides (TLCN-CP1, TLCN-CP2, and TLCN-CP3; underlines) used for the surface plasmon resonance analysis (Biacore 2000). Biotinylated peptides were immobilized on streptavidin-coated sensor chips, and recombinant GST-fusion proteins containing ezrin and radixin FERM domains (500 nM) were applied. The start and end points of injection of recombinant proteins are indicated by arrow and arrowhead, respectively. The juxtamembrane sequence of TLCN cytoplasmic region specifically binds the FERM domains of ezrin and radixin. ***B***, Specificity and kinetics of binding between TLCN and ERM proteins. Biotinylated ICAM-2-CP1, TLCN-CP1, and mutated TLCN-CP1 peptides were immobilized on streptavidin-coated sensor chips, and serially diluted recombinant GST-fusion proteins containing various FERM domains (1000, 500, 250, 125, and 62.5 nM) were applied. ***C***, Bar graphs summarizing the maximal resonance units for individual interactions between ICAM-2 or TLCN peptides and FERM domains. Error bars indicate SD ($n = 3$).

shows significant homology to those of other ERM-binding molecules (Fig. 1*C*).

The interaction between TLCN and ERM FERM domains was confirmed by yeast two-hybrid analysis, using ICAM-2 as a positive control. The full-length TLCN-CR interacted with the FERM domains of ezrin, radixin, and moesin but not with those of merlin, band 4.1, and talin, whereas ICAM-2 bound also to band 4.1 as well as ezrin, radixin, and moesin (Fig. 1*D*).

Detailed binding properties between TLCN and ERM proteins

Surface plasmon resonance analysis (Biacore) for measurement of direct protein–protein interaction was performed to further confirm the specific binding between TLCN and ERM proteins. Biotinylated synthetic peptides corresponding to distinct but overlapping sequences of the TLCN cytoplasmic region (TLCN-CP1, TLCN-CP2, and TLCN-CP3) (Fig. 2*A*) were immobilized on streptavidin-coated sensor tip and analyzed for interaction with recombinant GST-tagged FERM domains of ezrin and radixin. Specific binding to ezrin and radixin was observed only for the membrane-proximal TLCN-CP1 peptide but not for the middle TLCN-CP2 and C-terminal TLCN-CP3 peptides (Fig. 2*A*). The result clearly demonstrates that the juxtamembrane region of TLCN cytoplasmic domain is a binding site for ERM proteins.

Binding specificity and kinetics between TLCN and ERM proteins were analyzed using Biacore system (Fig. 2*B*,*C*). TLCN-CP1 peptide strongly bound to the FERM domains of ezrin and radixin with high affinities (K_D of 0.160 ± 0.017 and 0.359 ± 0.105 μM, respectively) but not to those of moesin, merlin, band 4.1, and talin. In contrast, ICAM-2 cytoplasmic peptide (ICAM-2-CP1) showed significant binding to all the FERM domains tested. Comparing the kinetics between TLCN-CP1 and ICAM-2-CP1, the association rate constants of radixin (500 nM)-binding to TLCN (6.42×10^4 M^{-1} s^{-1}) and ICAM-2 (6.67×10^4 M^{-1} s^{-1}) were almost the same, whereas the dissociation rate constant to TLCN (1.01×10^{-2} s^{-1}) was much faster than that to ICAM-2 (3.55×10^{-3} s^{-1}). This finding suggests that ICAM-2 firmly and stably binds to ERM proteins, whereas the binding between TLCN and ERM proteins may be more labile and easily dissociated.

When the four amino acids (Lys864, Lys865, Tyr868, and Val870) of TLCN corresponding to those of ICAM-2 that are crucial for binding to radixin (Hamada et al., 2003) were substituted to Ala to generate mutated TLCN-CP1 peptide, no significant binding activity was detected between mutated TLCN-CP1 and all the FERM domains. These results sug-

gest that TLCN and ICAM-2 share the similar binding mechanism to ERM proteins.

TLCN induces phosphorylated ERM-containing filopodia-like protrusions in N2a cells

To explore the functional meaning of the TLCN–ERM interaction, we established an ectopically TLCN-expressing neuroblastoma cell line (TLCN-N2a) in which the induction of TLCN expression is tightly regulated under the control of *E. coli lac* operon. Neither endogenous nor leaky appearance of TLCN was detectable in TLCN-N2a cells without IPTG. In contrast, the addition of IPTG to culture medium switched on the TLCN expression, which was first detected at 24 h and reached a maximal level at 72 h as assessed by Western blot analysis (Fig. 3*A*).

The interaction between TLCN and ezrin FERM domain in TLCN-N2a cells was analyzed by immunoprecipitation method. The TLCN-N2a cells were transfected with FLAG-tagged ezrin FERM domain-expressing plasmid, followed by the IPTG-induced expression of TLCN. Immunoprecipitation of TLCN from the cell lysate with anti-TLCN/Fc antibody resulted in coprecipitation of FLAG-tagged ezrin FERM domain, demonstrating the physical interaction between TLCN and FERM domain in mammalian cells (Fig. 3*B*).

ERM proteins are mostly present in cytoplasm in an inactive form and only become activated during phosphorylation of a Thr residue near the C terminus (Nakamura et al., 1995; Hayashi et al., 1999). Phosphorylated active forms of ERM proteins (phospho-ERM) bind to membrane proteins through the N-terminal FERM domain and to actin cytoskeleton through the C-terminal domain and induce the formation of specialized membrane protrusion structures such as microvilli, membrane ruffles, and uropods (Tsukita and Yonemura, 1999; Bretscher et al., 2002). When TLCN was ectopically expressed in N2a cells, a dramatic alteration in cellular morphology was observed: from small and round shape of control cells (Fig. 3*C–F*) to spreading morphology of TLCN-expressing cells bearing multiple filopodia-like protrusions (Fig. 3*G–V*). These protrusions contained phospho-ERM together with TLCN and F-actin (Fig. 3*G–J*).

Phospho-ERM proteins associate with plasma membrane by binding to membrane phosphoinositide, phosphatidylinositol-(4,5)bisphosphate [PI(4,5)P_2], through the FERM domain (Tsukita and Yonemura,

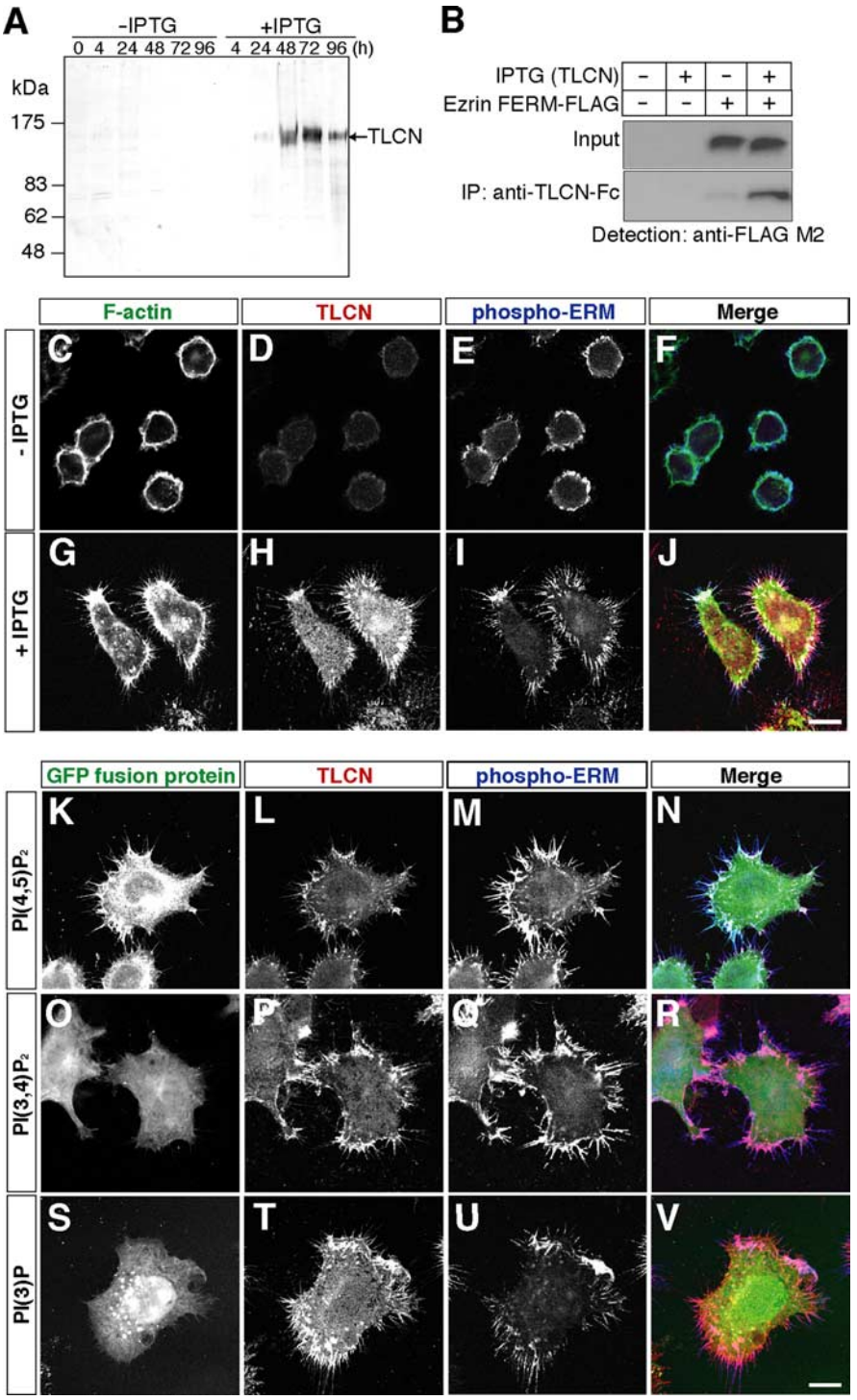

Figure 3. TLCN induces phospho-ERM-containing filopodia-like protrusions in N2a cells. ***A***, Western blot analysis for the time course of TLCN expression induced by IPTG in TLCN-N2a cells. ***B***, Coimmunoprecipitation of TLCN with FLAG-tagged ezrin FERM domain in TLCN-N2a cells. TLCN-N2a cells were transfected with control or FLAG-tagged ezrin FERM domain-expressing plasmids in the presence or absence of IPTG, lysed, immunoprecipitated with anti-TLCN/Fc antibody, and immunoblotted with anti-FLAG M2 antibody. Input indicates the lysate of cells subjected to immunoprecipitation. ***C–J***, Triple labeling of TLCN/N2a cells in the absence (***C***, ***F***, ***G***, ***J***) or presence (***G–J***) of IPTG with rhodamine–phalloidin (***C***, ***F***, ***G***, ***J***; green), anti-TLCN antibody (***D***, ***F***, ***H***, ***J***; red), and anti-phospho-ERM antibody (***E***, ***F***, ***I***, ***J***; blue). Merged images are shown in ***F*** and ***J***. TLCN expression induces the formation of filopodia-like protrusions containing F-actin and phospho-ERM. ***K–V***, Comparison of localizations of phosphoinositides (***K***, ***N***, ***O***, ***R***, ***S***, ***V***; green), TLCN (***L***, ***N***, ***P***, ***R***, ***T***, ***V***; red), and phospho-ERM (***M***, ***N***, ***Q***, ***R***, ***U***, ***V***; blue) in TLCN/N2a cells in the presence of IPTG. Merged images are shown in ***N***, ***R***, and ***V***. Localizations of phosphoinositides were visualized by transfection of plasmids expressing fluorescent probes, PLCδ1-PH–GFP (***K***, ***N***), TAPP2-PH–GFP (***O***, ***R***), and EEA1–3×–FYVE–GFP (***S***, ***V***), that are specific for PI(4,5)P_2, PI(3,4)P_2, and PI(3)P, respectively (Balla and Varnai, 2002). Only PI(4,5)P_2 is colocalized in TLCN-induced phospho-ERM-containing filopodia-like protrusions. Scale bars, 10 μm.

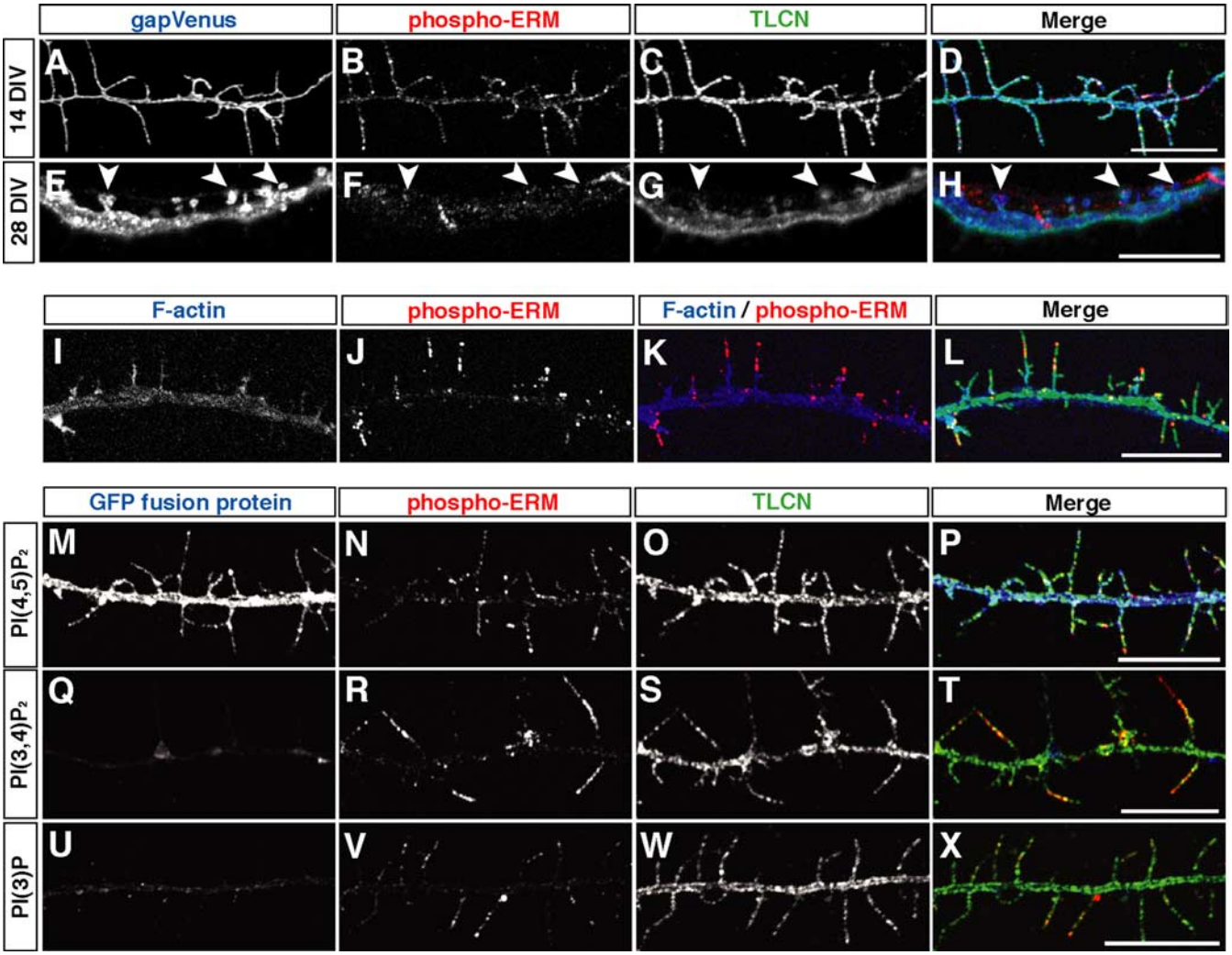

Figure 4. TLCN colocalizes with phospho-ERM in hippocampal neurons. ***A–H***, Triple immunolabeling of gapVenus-expressing cultured hippocampal neurons at 14 DIV (***A–D***) and 28 DIV (***E–H***) with anti-GFP (***A***, ***D***, ***E***, ***H***; blue), anti-phospho-ERM (***B***, ***D***, ***F***, ***H***; red), and anti-TLCN (***C***, ***D***, ***G***, ***H***; green) antibodies. Merged images are shown in ***D*** and ***H***. ***I–L***, Triple labeling of 14 DIV hippocampal neurons with rhodamine–phalloidin (***I***, ***K***, ***L***; blue), anti-phospho-ERM antibody (***J***, ***K***, ***L***; red), and anti-TLCN antibody (***L***; green). Merged image are shown in ***K*** and ***L***. F-actin and phospho-ERM are detected in dendritic filopodia but show distinct localizations; F-actin in proximal and phospho-ERM in distal segments. ***M–X***, Comparison of localizations of phosphoinositides [$PI(4,5)P_2$ in ***M*** and ***P***; $PI(3,4)P_2$ in ***Q*** and ***T***; PI(3)P in ***U*** and ***X***; blue], phospho-ERM (***N***, ***P***, ***R***, ***T***, ***V***, ***X***; red), and TLCN (***O***, ***P***, ***S***, ***T***, ***W***, ***X***; green) in hippocampal neurons. Merged images are shown in ***P***, ***T***, and ***X***. Dendritic filopodia contain $PI(4,5)P_2$ together with phospho-ERM and TLCN but not $PI(3,4)P_2$ and PI(3)P. Scale bars, 10 μm.

1999; Bretscher et al., 2002). We investigated the intracellular localization of $PI(4,5)P_2$, $PI(3,4)P_2$, and PI(3)P in TLCN-N2a cells by expressing individual phosphoinositide-specific fluorescent probes: PLCδ1-PH–GFP, TAPP2-PH–GFP, and EEA1–3×-FYVE–GFP, respectively (Balla and Varnai, 2002). Among the three phosphoinositides, only $PI(4,5)P_2$ visualized with PLCδ1-PH–GFP was present in the filopodia-like protrusions, colocalizing with TLCN and phospho-ERM (Fig. 3*K–N*). In contrast, TAPP2-PH–GFP was found diffusely in the cytoplasm (Fig. 3*O–R*), and EEA1–3×–FYVE–GFP was detected mainly in the intracellular granules and nuclei (Fig. 3*S–V*), indicating that $PI(3,4)P_2$, and PI(3)P are not colocalized with TLCN and phospho-ERM.

Together, the ectopic expression of TLCN in N2a cells induced filopodia-like protrusions that contain $PI(4,5)P_2$, phospho-ERM, F-actin, and TLCN itself.

Phospho-ERM proteins colocalize with TLCN in dendritic filopodia of hippocampal neurons

Next, we investigated the localization of phospho-ERM proteins in cultured hippocampal neurons in which endogenous TLCN is expressed abundantly in dendritic filopodia, shafts, and cell bodies but hardly in mature spines and not in axons (Matsuno et al., 2006). At 14 d *in vitro* (DIV), most of the dendritic protrusions are filopodia as visualized by the expression of membrane-tagged YFP derivative (gapVenus) (Fig. 4*A–D*). At this developmental stage, phospho-ERM clusters were detected predominantly in dendritic filopodia and colocalized with TLCN (Fig. 4*A–D*). At 28 DIV, in contrast, most dendritic filopodia turn into mushroom-shaped spines (Fig. 4*E–H*, arrowheads). Phospho-ERM and TLCN were mostly excluded from these spines (Fig. 4*E–H*). These results suggest that the functional interaction between phospho-ERM and TLCN can take place in dendritic filopodia but not in mature spines.

Similar to the phospho-ERM-containing filopodia-like protrusions in TLCN-expressing N2a cells, the dendritic filopodia in hippocampal neurons also contained F-actin (Fig. 4*I–L*) and $PI(4,5)P_2$ (Fig. 4*M–P*) but not $PI(3,4)P_2$ and PI(3)P (Fig. 4*Q–X*). However, a detailed comparison of phospho-ERM and F-actin signals in dendritic filopodia revealed differential localization:

phospho-ERM in a distal segment and F-actin in a proximal segment of filopodia (Fig. 4*I–L*).

Recently, Nyman-Huttunen et al. (2006) reported that TLCN binds to another actin-binding protein, α-actinin. To compare the localizations of TLCN, phospho-ERM, and α-actinin in hippocampal neurons, we performed triple immunofluorescence labeling (Fig. 5). Although both phospho-ERM and α-actinin showed colocalization with TLCN, their subcellular distributions appeared mutually exclusive. α-Actinin was mostly detected in cell bodies as well as dendritic shafts (Fig. 5*C*,*G*,*K*), whereas phospho-ERM was mainly localized to dendritic filopodia (Fig. 5*B*,*F*,*J*). These results suggest that TLCN properly uses two types of actin-binding proteins, ERM and α-actinin, to execute different functions linked to actin cytoskeleton in distinct subcellular domains, dendritic filopodia and cell bodies, respectively.

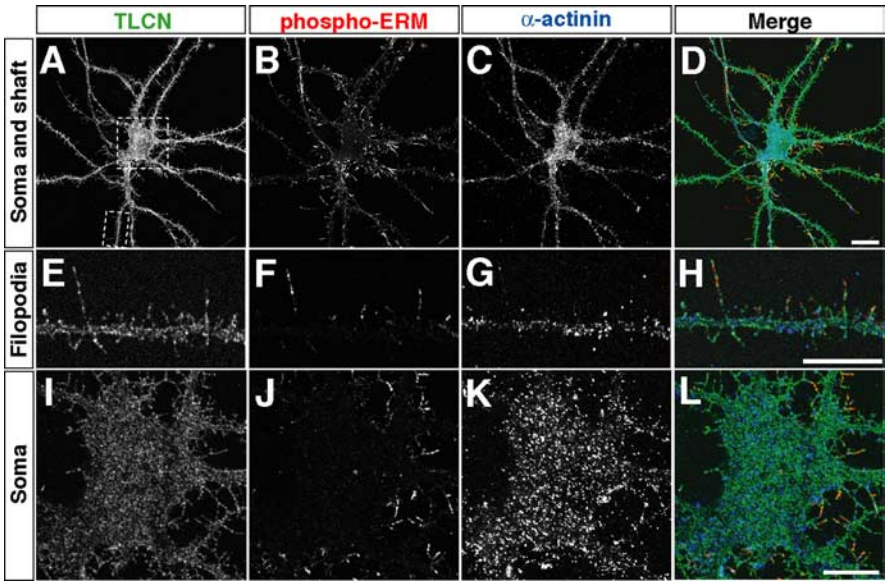

Figure 5. Colocalization of TLCN with phospho-ERM and α-actinin in distinct subcellular domains of hippocampal neurons. ***A–L***, Triple immunofluorescence labeling of hippocampal neurons (14 DIV) with antibodies against TLCN (***A***, ***D***, ***E***, ***H***, ***I***, ***L***; green), phospho-ERM (***B***, ***D***, ***F***, ***H***, ***J***, ***L***; red), and α-actinin (***C***, ***D***, ***G***, ***H***, ***K***, ***L***; blue). ***E–L***, Higher-magnification images of a dendrite (***E–H***) and a soma (***I–L***) (indicated as dashed squares in ***A***). Phospho-ERM is preferentially localized to dendritic filopodia (***F***, ***H***), whereas α-actinin is mostly distributed in soma and dendritic shafts (***G***, ***H***, ***K***, ***L***). Scale bars: ***D***, 20 μm; ***H***, ***L***, 10 μm.

Active ezrin induces dendritic filopodia formation in hippocampal neurons

Overexpression of TLCN causes a dramatic increase in the number of dendritic filopodia in hippocampal neurons (Matsuno et al., 2006). Because TLCN interacts with ERM FERM domains and is colocalized with phospho-ERM in dendritic filopodia, we hypothesized that the activation of ERM proteins would facilitate the formation of dendritic filopodia. To examine this possibility, we analyzed the dendritic morphology of 14 DIV hippocampal neurons expressing a constitutively active form of ezrin (ezrin–T567D) in which Thr567 near the C terminus was substituted to Asp to mimic phosphorylated Thr in the active state of ezrin (Gautreau et al., 2000). The density of dendritic filopodia in ezrin–T567D-expressing neurons was remarkably higher than that in control neurons (Fig. 6*A–C*). In addition, the ezrin–T567D-expressing neurons had significantly longer dendritic filopodia (Fig. 6*D*). The mean protrusion lengths were 2.35 ± 0.05 μm for control and 3.50 ± 0.06 μm for ezrin–T567D-expressing neurons. These results corroborate the idea that ERM proteins are involved in the morphogenesis of dendritic filopodia and that the activation of ERM proteins facilitate the elongation of dendritic filopodia.

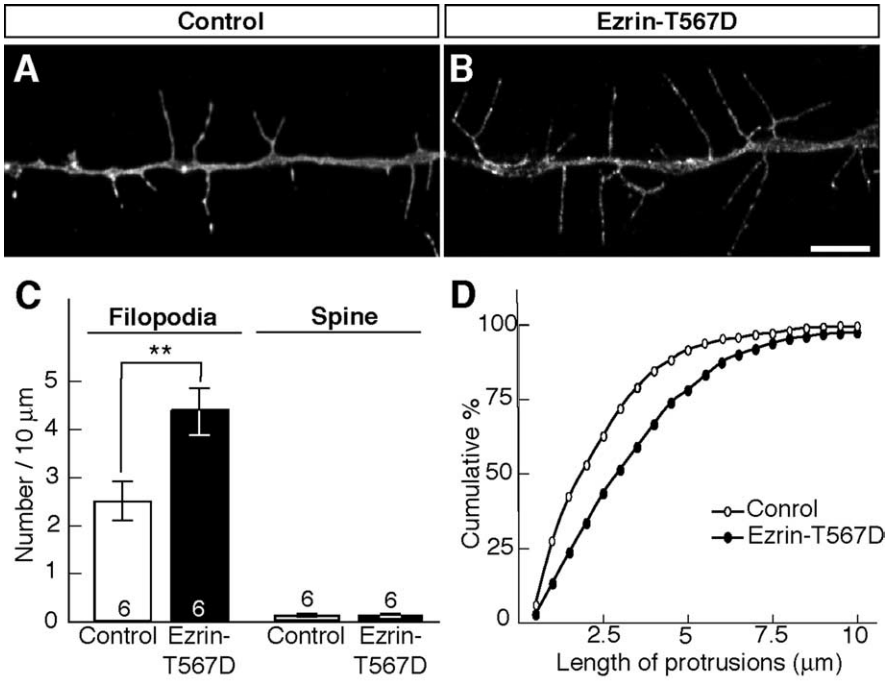

Figure 6. Constitutively active ezrin enhances dendritic filopodia formation. Hippocampal neurons (12 DIV) were injected with control (***A***) and ezrin–T567D-expressing (***B***) plasmids, together with gapVenus expressing-plasmid to visualize fine dendritic morphology. The neurons were stained with anti-GFP antibody at 14 DIV. ***A***, ***B***, Representative dendritic morphology of control and ezrin–T567D-expressing neurons. Ezrin–T567D-expressing neurons have more numerous and longer dendritic filopodia than control neurons. Scale bar, 5 μm. ***C***, Densities of filopodia and spines in control ($n = 6$) and ezrin–T567D-expressing ($n = 6$) neurons. $^{**}p < 0.01$, two-tailed Student's *t* test. Error bars indicate SEM. ***D***, Cumulative frequency plots for dendritic protrusion length in control (open circles) and ezrin–T567D-expressing (filled circles) neurons.

Knockdown of ERM proteins causes malformation of dendritic filopodia

To further examine the crucial role of ERM proteins in dendritic filopodia formation and elongation, we next performed siRNA-mediated knockdown of ERM proteins in cultured hippocampal neurons. siRNA-expressing plasmids were designed and constructed for ezrin, radixin, and moesin, and their effects were first assessed in N2a cells by quantitative reverse transcription-PCR and Western blot analyses. Expression levels of individual ERM

mRNAs and proteins were greatly reduced by ~80% during expression of ezrin, radixin, and moesin siRNAs (supplemental Fig. 1*A*,*B*, available at www.jneurosci.org as supplemental material). The hippocampal neurons were injected with a mixture of three plasmids expressing ezrin, radixin, and moesin siRNA or a control plasmid at 12 DIV. In ERM siRNA mix-expressing hippocampal neurons, the staining intensity of phospho-ERM proteins was greatly reduced compared with neighboring control neurons (supplemental Fig. 1*C*, available at www.jneurosci.org as supplemental material).

siRNA-mediated triple knockdown of all ERM proteins resulted in a marked decrease in filopodia density and a concomitant increase in spine density at the 14 DIV hippocampal neurons (Fig. 7*A–D*). This effect accompanied with a significant reduction in the length of dendritic protrusions (Fig. 7*E*). The mean lengths of protrusions were 2.14 ± 0.03 μm for control siRNA and 1.73 ± 0.02 μm for ERM siRNA mix.

Next, we examined the effects of double knockdown of ERM family members on filopodia formation and spine maturation. Hippocampal neurons at 12 DIV were transfected with three combinations of two siRNA-expressing plasmids: ezrin/radixin (ER), ezrin/moesin (EM), or radixin/moesin (RM). The filopodia density was decreased dramatically by RM double knockdown to the level of ERM triple knockdown and moderately by ER double knockdown, whereas EM double knockdown had little effect (Fig. 7*C*). In contrast, the spine maturation was significantly accelerated by double knockdowns of ER or EM, whereas RM double knockdown showed no significant effect (Fig. 7*D*). These results suggest the differential actions of ERM proteins at distinct steps in morphogenesis of dendritic protrusions. The filopodia formation is enhanced by the synergistic actions of radixin and moesin, whereas the spine maturation is regulated mainly by ezrin.

In summary, the density and length of dendritic filopodia were increased by the expression of constitutively active ezrin (gain-of-function) (Fig. 6), whereas they were decreased by the siRNA-mediated knockdown of ERM proteins (loss-of-function) (Fig. 7). Thus, ERM proteins play a crucial role in the morphological and functional maturation of dendritic protrusions in developing neurons.

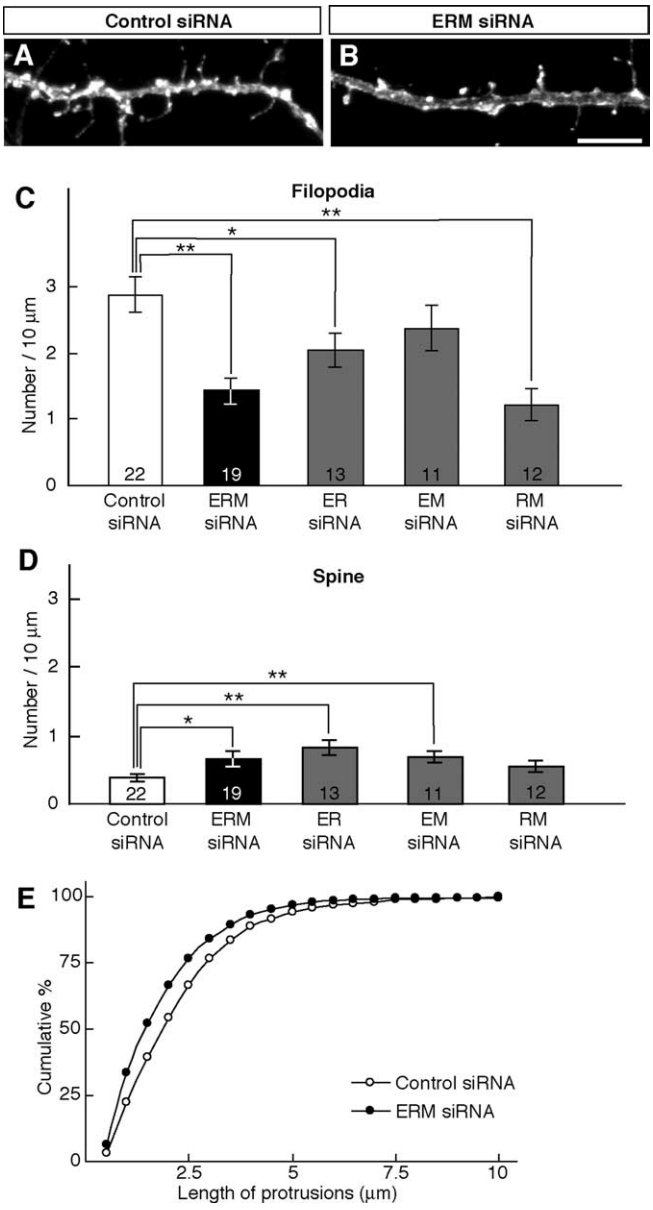

Figure 7. ERM knockdown causes malformation of dendritic filopodia. Hippocampal neurons (12 DIV) were injected with 0.75 μg/μl control siRNA-expressing (***A***), 0.25 μg/μl each of ezrin/radixin/moesin siRNA-expressing (***B***; ERM siRNA mix), ezrin/radixin/control, ezrin/moesin/control, and radixin/moesin/control siRNA-expressing (ER, EM, and RM siRNA mix) plasmids, together with 0.05 μg/μl gapVenus expression plasmid. The neurons were stained with anti-GFP antibody at 14 DIV. ***A***, ***B***, Representative dendritic morphology of control siRNA- and ERM siRNA mix-expressing neurons. ERM siRNA mix-expressing neurons show the decrease in filopodia number and the acceleration of spine maturation. Scale bar, 5 μm. ***C***, ***D***, Densities of filopodia (***C***) and spines (***D***) in control siRNA-expressing (white bars; $n = 22$), ERM siRNA mix-expressing (black bars; $n = 19$), ER siRNA mix-expressing (gray bars; $n = 13$), EM siRNA mix-expressing (gray bars; $n = 11$), and RM siRNA mix-expressing (gray bars; $n = 12$) neurons. $^*p < 0.05$ and $^{**}p < 0.01$, two-tailed Student's *t* test. Error bars indicate SEM. ***E***, Cumulative frequency plot for dendritic protrusion length in control siRNA-expressing (open circles) and ERM siRNA mix-expressing (filled circles) neurons.

Discussion

TLCN facilitates the formation and maintenance of dendritic filopodia and slows spine maturation (Matsuno et al., 2006). In the present study, we investigated the intracellular molecular cascade that leads to the TLCN-induced dendritic filopodia formation and obtained the following results. (1) The juxtamembrane cytoplasmic region of TLCN binds to the FERM domain of ERM family proteins. (2) Ectopic expression of TLCN induces phospho-ERM-containing filopodia-like protrusions in N2a cells. (3) Phospho-ERM proteins are colocalized with TLCN in dendritic filopodia and excluded from mature spines of hippocampal neurons. (4) Expression of constitutively active ezrin induces dendritic filopodia formation and elongation. (5) siRNA-mediated knockdown of ERM proteins reduces length and density of dendritic filopodia and accelerates spine maturation. These results demonstrate that the interaction between TLCN and activated ERM is a crucial step for the formation and elongation of dendritic filopodia in neurons.

We propose a model (Fig. 8) for possible functions of active and inactive forms of ERM proteins as TLCN-interacting molecules in dendritic filopodia formation and spine maturation. TLCN (green) is abundantly present on the plasma membrane of neuronal dendrites. ERM proteins in the cytoplasm are converted from inactive forms (blue) to active forms (red) through phosphorylation. The phospho-ERM proteins then bind to TLCN, enhance the formation and maintenance of dendritic filopodia, and thereby slow spine maturation. For transformation from dendritic filopodia to spines, ERM proteins are dephosphorylated, TLCN is excluded from spines, and several cell recognition molecules (N-cadherin/catenins, Ephs/ephrins, and syndecan-2)

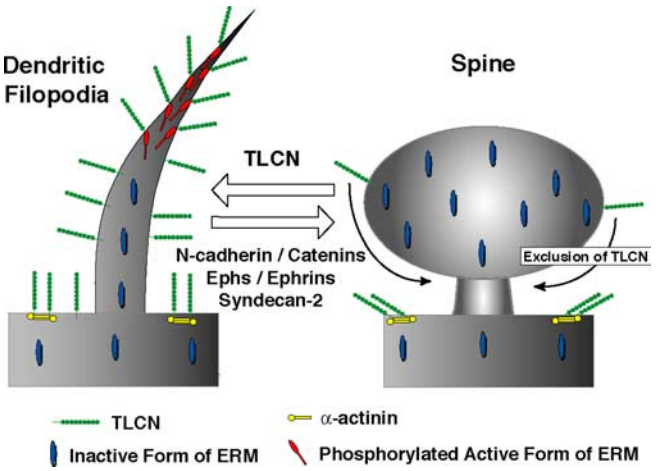

Figure 8. A model for the role of TLCN–ERM interaction in dendritic filopodia. In dendritic filopodia, ERM proteins are phosphorylated to become the active form (red) that can bind TLCN (green) in the plasma membrane. In dendritic shafts and spines, inactive ERM proteins (blue) are diffusely present in cytoplasm. Conversely, α-actinin (yellow) constantly binds TLCN in dendritic shafts. The interaction between TLCN and phospho-ERM mediates the formation, elongation, and maintenance of dendritic filopodia and slows spine maturation, whereas N-cadherin/catenins, Ephs/ephrins, and syndecan-2 enhance stabilization of mature synapses.

facilitate spine maturation and synapse stabilization (Ethell and Pasquale, 2005). Thus, the ERM proteins may play an important role as a phosphorylation-dependent molecular switch that regulates morphological and functional transformation between dendritic filopodia and spines.

Ins and outs of telencephalin

TLCN is a type I integral membrane glycoprotein specifically expressed in spiny neurons within the mammalian telencephalon (Yoshihara et al., 1994). The cytoplasmic region of TLCN consists of ~60 amino acids that are highly conserved across various mammalian species. Recently, we reported that the TLCN cytoplasmic region is required for both its directional targeting into dendrites and its function of dendritic filopodia formation (Mitsui et al., 2005; Matsuno et al., 2006). In this study, we identified ERM family proteins as the intracellular binding partners of TLCN that mediate the dendritic filopodia formation. The binding site of ERM proteins locates in the juxtamembrane domain of TLCN cytoplasmic region whose amino acid sequence closely resembles the ERM-binding sites of other membrane proteins. In particular, several crucial amino acid residues in ICAM-2 for radixin binding identified by co-crystallographic analysis (Hamada et al., 2003) are perfectly conserved in TLCN. Based on the alignment of seven representative ERM-binding proteins including TLCN and ICAM-2 (Fig. 1*C*), a consensus motif important for the ERM binding may be defined as [transmembrane region] − [5–7 amino acids with 2–4 basic residues] -Gly-X-Tyr-X-Val/Leu-X-Glu-Ala-.

Recently, Nyman-Huttunen et al. (2006) reported an interaction between TLCN cytoplasmic region and another actin-binding protein, α-actinin. We made a detailed comparison of distribution patterns of α-actinin and phospho-ERM in cultured hippocampal neurons (Fig. 5) and found that they are colocalized with TLCN in distinct subcellular domains in a mutually exclusive manner. α-Actinin is mostly present in cell bodies and dendritic shafts, whereas phospho-ERM is localized to dendritic filopodia. Because α-actinin binds also to the cytoplasmic region of integrins (Otey and Carpen, 2004), a tertiary complex comprising TLCN, α-actinin, and integrin may be formed and contribute to stable adhesion of neuronal cell bodies and dendritic shafts to extracellular matrix proteins. Surface plasmon resonance analysis revealed that TLCN binds to the FERM domains of ezrin and radixin with relatively high affinities (K_D of 0.160 and 0.359 μM, respectively) (Fig. 2). In contrast, the binding affinity between TLCN and α-actinin was reported to be much lower by two orders of magnitude (K_D of 22.9 μM) (Nyman-Huttunen et al., 2006). These findings suggest that TLCN might use two types of actin-binding proteins, phospho-ERM and α-actinin, in distinct subcellular domains and for different functions: the stronger binding of TLCN with phospho-ERM may lead to the formation and elongation of dendritic filopodia, whereas weaker binding of TLCN with α-actinin at the soma and dendritic shafts might mediate the cell-substrate adhesion.

TLCN-induced formation of dendritic filopodia requires the extracellular region of TLCN as well as the cytoplasmic region (Matsuno et al., 2006), suggesting the presence of a ligand or a counter-receptor for TLCN. What molecule triggers the TLCN-mediated filopodia formation? The extracellular region of TLCN consists of nine Ig-like domains that potentially interact with multiple ligands or counter-receptors. To date, two molecules have been identified as counter-receptors for TLCN: (1) lymphocyte function-associated antigen-1 (LFA-1) on leukocytes and microglia (Mizuno et al., 1997; Tian et al., 1997) and (2) TLCN itself on neuronal dendrites (Tian et al., 2000). It is unlikely that these two types of interactions play a role in dendritic filopodia formation, because LFA-1-expressing microglia are not contained in our culture condition and because dendritic filopodia arise without any contact to other dendrites. Additional studies are needed to search for molecules that may be present in the extracellular matrix or on the axonal membrane, bind to the extracellular region of TLCN, and facilitate the dendritic filopodia formation.

ERM proteins in dendritic filopodia

Dendritic filopodia are highly dynamic protrusions abundantly found in immature neurons during development including a "critical period" of neural circuit formation and refinement (Hensch, 2005). Dendritic filopodia behave as if they are searching for appropriate synaptic partners and are morphologically and functionally converted into mature spines during the right choice of target axons. Compared with a wealth of knowledge on molecular constituents in spines (Yamagata et al., 2003; Tada and Sheng, 2006), only a limited number of molecules have been identified that are present in dendritic filopodia, such as TLCN, F-actin, and drebrin (Zhang and Benson, 2002; Mizui et al., 2005; Matsuno et al., 2006). Here we add a new important player, phospho-ERM, in this group. Compared with other molecules that are also distributed in dendritic shafts, the localization of phospho-ERM is highly specific to filopodia, thus providing a useful and reliable molecular marker of dendritic filopodia. In addition, the gain-of-function experiment with constitutively active ezrin and the loss-of-function experiment by siRNA-mediated ERM knockdown provided direct evidence for the functional importance of ERM proteins in dendritic filopodia formation and elongation.

Members of the ERM family link integral plasma-membrane proteins with underlying actin cytoskeleton, participate in signal transduction pathways, and mediate the formation of specialized membrane protrusions such as microvilli, uropods, and ruffles (Tsukita and Yonemura, 1999; Bretscher et al., 2002). ERM proteins are mostly located in the cellular cytoplasm as an inactive

form through the intramolecular association between their N-terminal and C-terminal domains. The functional activation of ERM proteins is triggered by two factors: (1) the phosphorylation of a Thr residue near the C terminus and (2) the presence of $PI(4,5)P_2$ in the plasma membrane. We found that dendritic filopodia contain TLCN, $PI(4,5)P_2$, phospho-ERM, and F-actin, all of which presumably play important roles in the signal transduction cascade leading to the formation and maintenance of dendritic filopodia. One of the important steps toward the molecular dissection of dendritic filopodia would be to identify a crucial protein kinase that mediates the phosphorylation of ERM proteins. Although several kinases are reported to be capable of phosphorylating ERM proteins such as Rho-associated kinase, protein kinase Cα, protein kinase Cθ, Nck-interacting kinase, and myotonic dystrophy kinase-related cell division cycle 42-binding kinase (Matsui et al., 1998; Oshiro et al., 1998; Pietromonaco et al., 1998; Nakamura et al., 2000; Ng et al., 2001; Bretscher et al., 2002; Baumgartner et al., 2006), their expression in neurons, particularly in dendritic filopodia, has not been investigated so far.

The localization of phospho-ERM in dendritic filopodia showed two intriguing characteristics. First, the staining pattern with anti-phospho-ERM antibody is different from filopodia to filopodia: some are strongly positive for phospho-ERM, whereas the others show weak or no appearance. Such a nonhomogeneous labeling may reflect different states of dendritic filopodia such as elongating, retracting, pausing, or contacting with an axon. An invention of a specific fluorescent probe for detection of the active form of ERM proteins in living cells and its use for time-lapse imaging of dendritic filopodia dynamics will provide a useful tool to address this issue. Second, a close comparative examination revealed distinct localizations of phospho-ERM and F-actin in different subdomains of single dendritic filopodia: phospho-ERM proteins are mainly localized in the distal portion of dendritic filopodia, whereas F-actin is more abundantly present in the proximal portion. Recently, a similar observation has been reported in differential localization of phospho-ERM and F-actin in subdomains of microvilli (Hanono et al., 2006). Because the distal portion of dendritic filopodia and microvilli are considered to be highly dynamic, the activated ERM may be involved in either polymerization or depolymerization of F-actin, leading to elongation or retraction of dendritic filopodia.

The siRNA-mediated knockdown experiment of ERM proteins in hippocampal neurons yielded an unexpected result. The density of dendritic filopodia was most dramatically reduced by double knockdown of radixin and moesin, whereas the spine density was significantly increased by knockdown of ezrin. This finding indicates differential contributions of ERM family proteins at two distinct steps in morphogenesis of dendritic protrusions. Radixin and moesin may play a role in the formation of filopodia at an early step, whereas ezrin may negatively regulate the filopodia-to-spine transition at a late step. Although the molecular mechanism and functional significance of the specialization of ERM proteins in neurons remain to be elucidated, it would be interesting if TLCN properly uses three ERM proteins at appropriate steps during development.

Recently, several neuronal functions of ERM proteins have been reported. A functional binding between L1, an axonal adhesion molecule belonging to the Ig superfamily, and ERM proteins is involved in neurite branching during development and regenerative response to injury (Dickson et al., 2002; Haas et al., 2004; Cheng et al., 2005). In axonal growth cones, radixin and moesin regulate their morphology and motility (Paglini et al., 1998; Castelo and Jay, 1999). Also, activated radixin mediates $GABA_A$ receptor α5 subunit anchoring at actin cytoskeleton in dendritic shafts (Loebrich et al., 2006). Thus, together with the present finding on TLCN–ERM interaction in dendritic filopodia, ERM family proteins link multiple membrane proteins with actin cytoskeleton in distinct subcellular domains and play various important roles in morphogenesis of developing neurons and functional regulation of mature neurons.

References

Balla T, Varnai P (2002) Visualizing cellular phosphoinositide pools with GFP-fused protein-modules. Sci STKE 2002:L3.

Baumgartner M, Sillman AL, Blackwood EM, Srivastava J, Madson N, Schilling JW, Wright JH, Barber DL (2006) The Nck-interacting kinase phosphorylates ERM proteins for formation of lamellipodium by growth factors. Proc Natl Acad Sci USA 103:13391–13396.

Benson DL, Yoshihara Y, Mori K (1998) Polarized distribution and cell type-specific localization of telencephalin, an intercellular adhesion molecule. J Neurosci Res 52:43–53.

Bretscher A, Edwards K, Fehon RG (2002) ERM proteins and merlin: integrators at the cell cortex. Nat Rev Mol Cell Biol 3:586–599.

Castelo L, Jay DG (1999) Radixin is involved in lamellipodial stability during nerve growth cone motility. Mol Biol Cell 10:1511–1520.

Cheng L, Itoh K, Lemmon V (2005) L1-mediated branching is regulated by two ezrin-radixin-moesin (ERM)-binding sites, the RSLE region and a novel juxtamembrane ERM-binding region. J Neurosci 25:395–403.

Dailey ME, Smith SJ (1996) The dynamics of dendritic structure in developing hippocampal slices. J Neurosci 16:2983–2994.

Dickson TC, Mintz CD, Benson DL, Salton SR (2002) Functional binding interaction identified between the axonal CAM L1 and members of the ERM family. J Cell Biol 157:1105–1112.

Dunaevsky A, Tashiro A, Majewska A, Mason C, Yuste R (1999) Developmental regulation of spine motility in the mammalian central nervous system. Proc Natl Acad Sci USA 96:13438–13443.

Ethell IM, Pasquale EB (2005) Molecular mechanisms of dendritic spine development and remodeling. Prog Neurobiol 75:161–205.

Fiala JC, Feinberg M, Popov V, Harris KM (1998) Synaptogenesis via dendritic filopodia in developing hippocampal area CA1. J Neurosci 18:8900–8911.

Fromont-Racine M, Rain JC, Legrain P (2002) Building protein-protein networks by two-hybrid mating strategy. Methods Enzymol 350:513–524.

Gautreau A, Louvard D, Arpin M (2000) Morphogenic effects of ezrin require a phosphorylation-induced transition from oligomers to monomers at the plasma membrane. J Cell Biol 150:193–203.

Haas MA, Vickers JC, Dickson TC (2004) Binding partners L1 cell adhesion molecule and the ezrin-radixin-moesin (ERM) proteins are involved in development and the regenerative response to injury of hippocampal and cortical neurons. Eur J Neurosci 20:1436–1444.

Hamada K, Shimizu T, Yonemura S, Tsukita S, Tsukita S, Hakoshima T (2003) Structural basis of adhesion-molecule recognition by ERM proteins revealed by the crystal structure of the radixin-ICAM-2 complex. EMBO J 22:502–514.

Hanono A, Garbett D, Reczek D, Chambers DN, Bretscher A (2006) EPI64 regulates microvillar subdomains and structure. J Cell Biol 175:803–813.

Harris KM, Kater SB (1994) Dendritic spines: cellular specializations imparting both stability and flexibility to synaptic function. Annu Rev Neurosci 17:341–371.

Hayashi K, Yonemura S, Matsui T, Tsukita S (1999) Immunofluorescence detection of ezrin/radixin/moesin (ERM) proteins with their carboxyl-terminal threonine phosphorylated in cultured cells and tissues. J Cell Sci 112:1149–1158.

Hensch TK (2005) Critical period plasticity in local cortical circuits. Nat Rev Neurosci 6:877–888.

Kaufmann WE, Moser HW (2000) Dendritic anomalies in disorders associated with mental retardation. Cereb Cortex 10:981–991.

Lendvai B, Stern EA, Chen B, Svoboda K (2000) Experience-dependent plasticity of dendritic spines in the developing rat barrel cortex *in vivo*. Nature 404:876–881.

Loebrich S, Bahring R, Katsuno T, Tsukita S, Kneussel M (2006) Activated radixin is essential for $GABA_A$ receptor α5 subunit anchoring at the actin cytoskeleton. EMBO J 25:987–999.

Marshall AJ, Krahn AK, Ma K, Duronio V, Hou S (2002) TAPP1 and TAPP2 are targets of phosphatidylinositol 3-kinase signaling in B cells: sustained plasma membrane recruitment triggered by the B-cell antigen receptor. Mol Cell Biol 22:5479–5491.

Matsui T, Maeda M, Doi Y, Yonemura S, Amano M, Kaibuchi K, Tsukita S, Tsukita S (1998) Rho-kinase phosphorylates COOH-terminal threonines of ezrin/radixin/moesin (ERM) proteins and regulates their head-to-tail association. J Cell Biol 140:647–657.

Matsuno H, Okabe S, Mishina M, Yanagida T, Mori K, Yoshihara Y (2006) Telencephalin slows spine maturation. J Neurosci 26:1776–1786.

Mitsui S, Saito M, Hayashi K, Mori K, Yoshihara Y (2005) A novel phenylalanine-based targeting signal directs telencephalin to neuronal dendrites. J Neurosci 25:1122–1131.

Mitsui S, Saito M, Mori K, Yoshihara Y (2007) A transcriptional enhancer that directs telencephalon-specific transgene expression in mouse brain. Cereb Cortex 17:522–530.

Mizui T, Takahashi H, Sekino Y, Shirao T (2005) Overexpression of drebrin A in immature neurons induces the accumulation of F-actin and PSD-95 into dendritic filopodia, and the formation of large abnormal protrusions. Mol Cell Neurosci 30:630–638.

Mizuno T, Yoshihara Y, Inazawa J, Kagamiyama H, Mori K (1997) cDNA cloning and chromosomal localization of the human telencephalin and its distinctive interaction with lymphocyte function-associated antigen-1. J Biol Chem 272:1156–1163.

Mori K, Fujita SC, Watanabe Y, Obata K, Hayaishi O (1987) Telencephalon-specific antigen identified by monoclonal antibody. Proc Natl Acad Sci USA 84:3921–3925.

Nagai T, Ibata K, Park ES, Kubota M, Mikoshiba K, Miyawaki A (2002) A variant of yellow fluorescent protein with fast and efficient maturation for cell-biological applications. Nat Biotechnol 20:87–90.

Nakamura F, Amieva MR, Furthmayr H (1995) Phosphorylation of threonine 558 in the carboxyl-terminal actin-binding domain of moesin by thrombin activation of human platelets. J Biol Chem 270:31377–31385.

Nakamura N, Oshiro N, Fukata Y, Amano M, Fukata M, Kuroda S, Matsuura Y, Leung T, Lim L, Kaibuchi K (2000) Phosphorylation of ERM proteins at filopodia induced by Cdc42. Genes Cells 5:571–581.

Ng T, Parsons M, Hughes WE, Monypenny J, Zicha D, Gautreau A, Arpin M, Gschmeissner S, Verveer PJ, Bastiaens PI, Parker PJ (2001) Ezrin is a downstream effector of trafficking PKC-integrin complexes involved in the control of cell motility. EMBO J 20:2723–2741.

Niwa H, Yamamura K, Miyazaki J (1991) Efficient selection for high-expression transfectants with a novel eukaryotic vector. Gene 108:193–199.

Nyman-Huttunen H, Tian L, Ning L, Gahmberg CG (2006) α-actinin-dependent cytoskeletal anchorage is important for ICAM-5-mediated neuritic outgrowth. J Cell Sci 119:3057–3066.

Oka S, Mori K, Watanabe Y (1990) Mammalian telencephalic neurons express a segment-specific membrane glycoprotein, telencephalin. Neuroscience 35:93–103.

Okabe S, Miwa A, Okado H (1999) Alternative splicing of the C-terminal domain regulates cell surface expression of the NMDA receptor NR1 subunit. J Neurosci 19:7781–7792.

Oshiro N, Fukata Y, Kaibuchi K (1998) Phosphorylation of moesin by Rho-associated kinase (Rho-kinase) plays a crucial role in the formation of microvilli-like structures. J Biol Chem 273:34663–34666.

Otey CA, Carpen O (2004) α-actinin revisited: a fresh look at an old player. Cell Motil Cytoskeleton 58:104–111.

Paglini G, Kunda P, Quiroga S, Kosik K, Caceres A (1998) Suppression of radixin and moesin alters growth cone morphology, motility, and process formation in primary cultured neurons. J Cell Biol 143:443–455.

Pietromonaco SF, Simons PC, Altman A, Elias L (1998) Protein kinase C-θ phosphorylation of moesin in the actin-binding sequence. J Biol Chem 273:7594–7603.

Rain JC, Selig L, De Reuse H, Battaglia V, Reverdy C, Simon S, Lenzen G, Petel F, Wojcik J, Schachter V, Chemama Y, Labigne A, Legrain P (2001) The protein-protein interaction map of *Helicobacter pylori.* Nature 409:211–215.

Tada T, Sheng M (2006) Molecular mechanisms of dendritic spine morphogenesis. Curr Opin Neurobiol 16:95–101.

Tian L, Yoshihara Y, Mizuno T, Mori K, Gahmberg CG (1997) The neuronal glycoprotein telencephalin is a cellular ligand for the CD11a/CD18 leukocyte integrin. J Immunol 158:928–936.

Tian L, Kilgannon P, Yoshihara Y, Mori K, Gallatin WM, Carpen O, Gahmberg CG (2000) Binding of T lymphocytes to hippocampal neurons through ICAM-5 (telencephalin) and characterization of its interaction with the leukocyte integrin CD11a/CD18. Eur J Immunol 30:810–818.

Tsukita S, Yonemura S (1999) Cortical actin organization: lessons from ERM (ezrin/radixin/moesin) proteins. J Biol Chem 274:34507–34510.

Yamagata M, Sanes JR, Weiner JA (2003) Synaptic adhesion molecules. Curr Opin Cell Biol 15:621–632.

Yoshihara Y, Mori K (1994) Telencephalin: a neuronal area code molecule? Neurosci Res 21:119–124.

Yoshihara Y, Oka S, Nemoto Y, Watanabe Y, Nagata S, Kagamiyama H, Mori K (1994) An ICAM-related neuronal glycoprotein, telencephalin, with brain segment-specific expression. Neuron 12:541–553.

Yuste R, Bonhoeffer T (2004) Genesis of dendritic spines: insights from ultrastructural and imaging studies. Nat Rev Neurosci 5:24–34.

Zhang W, Benson DL (2002) Developmentally regulated changes in cellular compartmentation and synaptic distribution of actin in hippocampal neurons. J Neurosci Res 69:427–436.

Ziv NE, Smith SJ (1996) Evidence for a role of dendritic filopodia in synaptogenesis and spine formation. Neuron 17:91–102.